Calculated electronic structure of chromium surfaces and chromium monolayers on iron

R. H. Victora and L. M. Falicov
Materials and Molecular Research Division, Lawrence Berkeley Laboratory and Department of Physics, University of California, Berkeley, California 94720
(Received 28 January 1985)

A self-consistent calculation of the magnetic and electronic properties of the chromium (100) and (110) surfaces and of a chromium monolayer on the (100) and (110) iron surfaces is presented. It is found that (i) the (100) chromium surface is ferromagnetic with a greatly enhanced spin polarization (3.00 electrons); (ii) a substantial enhancement of the spin imbalance exists several (>5) layers into the bulk; (iii) the (110) chromium surface is antiferromagnetic with a large (2.31) spin imbalance; (iv) the (100) chromium monolayer on ferromagnetic iron is ferromagnetic, with a huge spin imbalance (3.63), and aligned antiferromagnetically with respect to the bulk iron; (v) the (110) chromium monolayer on ferromagnetic iron is also ferromagnetic, with a spin imbalance of 2.25 and antiferromagnetically aligned to the iron. The spin imbalance of chromium on iron (100) is possibly the largest of any transition-metal system.

I. INTRODUCTION

There is considerable current interest in the magnetism and related electronic properties of $3d$ transition-metal surfaces and overlayers. These metals exhibit itinerant magnetism: their magnetization derives from the itinerant d electrons. In moving down the Periodic Table from Ni, there is a decrease in the number of these d electrons (an increase in the number of d holes) and a consequent increase in the bulk magnetization[1] from 0.61 Bohr magnetons in Ni, to 1.72 in Co, and 2.22 in Fe. Beyond Fe lie the more complicated magnetic structures of Mn and Cr which display localized moments but no net magnetization. In all these elements, the itinerant nature of the d electrons makes the magnetic properties a sensitive function of local environment. Consequently, the presence of a dissimilar neighbor, as found in an interface, or the absence of some neighbors, as found at a surface, may cause considerable changes in the local magnetic properties.

Bulk chromium occurs in the body-centered-cubic structure with an antiferromagnetic (AF) ground state modulated by an incommensurable spin-density wave (SDW). The SDW is in one of the $\langle 100 \rangle$ directions with a wavelength of approximately 21 lattice spacings.[2] The magnetization at the maximum is 0.59 Bohr magnetons.[3] Experimentally it is found that the addition of small amounts (approximately 1%) of group VII impurities such as Mn produces a simple AF structure[4] with a magnetic moment of approximately 0.67 Bohr magnetons. In this structure atoms in the body-centered positions of the bcc lattice have spins pointing only in one direction; atoms in the corner positions have spins in the opposite direction.

This simple AF structure demands that $\langle 100 \rangle$ planes contain atoms of only one spin direction. Consequently, the (100) surface is expected to possess ferromagnetic order. Evidence of this planar ferromagnetism is found in the electron-capture spectroscopy results of Rau and Eichner.[5] Their sample, however, displayed a $c(2\times2)$ structure indicative of impurities, which may have affected their results. The (100) surface has been examined also by two angle-resolved photoemission experiments;[6,7] both find a surface state or resonance at an energy approximately 0.70 eV below the Fermi level. Unfortunately the experiments disagree on the symmetry of this feature.[8] Klebanoff *et al.*[7] also found a surface-related feature with a very small binding energy.

The (100) surface of chromium has also been examined theoretically[9–11] by means of a simple exchange interaction and a tight-binding approach which neglected the *sp* conduction electrons. Allan[9] finds that the surface magnetization is very large (2.8 Bohr magnetons) relative to the bulk and argues that this enhancement should penetrate into the bulk, decreasing by a factor (-0.5) per layer. (The negative sign refers to the AF.) Grempel[11] finds a surface spin polarization of 2.6 Bohr magnetons and a very high surface Curie temperature.

Feibelman and Hamann,[12] in an effort to explain the superconducting properties of Au-Cr-Au sandwich films,[13] performed paramagnetic calculations within the local-density formalism for Cr (100) surface and overlayer systems. Near the Fermi level they found a large feature in the Cr surface layer which remained substantially unaffected by the application of, for example, a gold overlayer.

The $\langle 110 \rangle$ planes cut the simple AF bcc lattice so that an equal number of up and down spins are encountered. The (110) surface should therefore be an AF one. There have been two photoemission experiments on the Cr (110) surface. The experiment of Johansson *et al.*[14] found no evidence of surface states; the later experiment of Wincott *et al.*[15] measured the dispersion of a surface state (binding energy of approximately 0.2 eV) along $\bar{\Delta}$. The periodicity of their spectra suggests an AF surface.

Stainless steel is the name given to a family of iron-based alloys which contain at least 12% chromium. Auger electron spectroscopy[16] shows that when a 304 stainless-steel sample (a common type) is heated, there is a

strong enhancement of the Cr concentration at the surface. This is in agreement with chromium's lower heat of crystal formation.[17] It is this enhanced concentration of Cr at the surface which, when oxidized, is influential in preventing the rusting of the steel.

In this paper we present results of calculations for the magnetic and electronic properties of the (100) and (110) surfaces of Cr, and for the systems consisting of a monolayer of Cr deposited on the Fe (100) and (110) surfaces. We use a Slater-Koster parametrized tight-binding scheme in which the one- and two-center integrals are fitted to the bulk band structure. The electron-electron interaction is treated self-consistently in a single-site approximation. This scheme has been previously used and has produced excellent agreement with both experimental data and state-of-the-art calculations.

II. CALCULATION

In this section we describe our calculations. In Sec. II A we describe the Hamiltonian and in Sec. II B we examine the numerical accuracy of our work and the possible errors introduced by our major approximations.

A. Hamiltonian

We take our Hamiltonian to be the sum of a one-electron term H_0 and an electron-electron interaction term $H_{e\text{-}e}$. For H_0 we choose the parametrized tight-binding scheme of Slater and Koster.[18] The Hamiltonian H_0 is written in terms of one- and two-center integrals, which are treated as parameters chosen to fit the bulk band structure. We use the calculated paramagnetic bulk band structure of Moruzzi *et al.*[19] for both chromium and iron. We include s, p, and d orbitals with interactions up to second-nearest neighbors. For the matrix elements between Cr and Fe we take the geometric mean of the respective Cr-Cr and Fe-Fe matrix elements. The two sets of intersite matrix elements are similar, so the results are insensitive to the precise scheme for choosing the Cr-Fe matrix elements.

For the Fe or Cr electron-electron interaction we use a single-site approximation which has been extensively discussed,[20].

$$H_{e\text{-}e}=\sum_{i\sigma\sigma'}\sum_{\alpha\beta\gamma\delta}U_{\alpha\beta\gamma\delta}c^{\dagger}_{i\alpha\sigma}c^{\dagger}_{i\beta\sigma'}c_{i\gamma\sigma'}c_{i\delta\sigma}\ , \tag{1}$$

where $c^{\dagger}_{i\alpha\sigma}$ creates an orbital of symmetry α and spin σ at site i.

We treat $H_{e\text{-}e}$ in the Hartree-Fock approach; we can, with some approximation, reduce $H_{e\text{-}e}$ to a simple form for the on-site potential shifts,

$$\begin{aligned}\Delta E_{d\nu\sigma}=&-\tfrac{1}{2}(U-J)\langle m_{d\nu\sigma}\rangle-J\langle m_{d\sigma}\rangle\\&+\tfrac{1}{2}(U-2U'+J)\langle n_{d\nu}-n^0_{d\nu}\rangle\\&+V_{sd}\langle n_s-n^0_s\rangle+V_{dd}\langle n_d-n^0_d\rangle\ ,\\ \Delta E_{s\sigma}=&V_{ss}\langle n_s-n^0_s\rangle+V_{sd}\langle n_d-n^0_d\rangle\ .\end{aligned} \tag{2}$$

Here, $\Delta E_{d\nu\sigma}$ is the on-site potential shift for a d orbital of symmetry ν and spin σ, measured relative to the value for the pure magnetic metal. By $m_{d\nu\sigma}$ we denote the spin polarization ($n_{d\nu\sigma}-n_{d\nu\bar{\sigma}}$) in the d orbital of symmetry ν at a given site, and

$$m_{d\sigma}\equiv\sum_{\nu}m_{d\nu\sigma}\ .$$

The total d occupancy at the site is denoted by

$$n_d\equiv\sum_{\nu d}n_{d\nu\sigma}\ ,$$

and the value for the respective pure metal is n^0_d. Quantities for s and p orbitals are similarly defined. In (2), s refers to the entire sp complex.

We define U as the on-site direct Coulomb integral between d orbitals of the same symmetry [rescaled by correlation effects (see below)], U' is the integral between d orbitals of different symmetry, and J is the exchange integral. We define $V_{dd}\equiv U'-0.5J$, which gives the effective (repulsive) interaction between d electrons, aside from magnetic effects. We similarly define an effective interaction V_{ss} among sp electrons, and V_{sd} between sp and d electrons. We neglect the on-site exchange integrals other than those between d orbitals. Atomic symmetry demands that $U=U'+2J$. The ratio U:J is taken to be 5:1 as suggested by Herring.[21] The absolute magnitude of U is scaled to give the correct bulk magnetization $\mu=0.67\mu_B$ for simple AF chromium and $\mu=2.22\mu_B$ for iron. We use Auger-electron-spectroscopy data for Fe to set V_{dd} for both elements. The negligible charge rearrangement between paramagnetic and antiferromagnetic Cr, even when $V_{dd}=0$, demonstrates that the slight inaccuracy in the value of V_{dd} for chromium is not important.

It is difficult within the tight-binding approximation to treat charge transfer accurately at the surface. To avoid this problem and still treat charge transfer and potential shifts at the surface in a simple way, we impose upon our potential the constraint

$$\Delta n_{sp}=\Delta n_d=0\ . \tag{3}$$

That is, the average on-site potentials of the d orbitals and of the s and p orbitals are fixed by the requirement that the total occupancies of the sp and d complexes at any site should not differ from the bulk values. More fully self-consistent calculations[22–24] suggest that the d band gains or loses no more than 0.1 electrons at the surface. By neglecting this, we may expect to alter the calculated surface magnetization by less than a tenth of a Bohr magneton per atom, an acceptable level of error.

We calculated the total energy of each self-consistent state using the well-known formula[25]

$$E=\sum_{n\mathbf{k}}\left[\epsilon_{\mathbf{k}}-\tfrac{1}{2}\sum_{n'\mathbf{k}'}H_{e\text{-}e}\right], \tag{4}$$

where $\epsilon_{\mathbf{k}}$ is the one-particle removal energy and the sums are performed over the occupied states. The nonintuitive term involving $H_{e\text{-}e}$ corrects for the double counting of the electron-electron interaction.

B. Accuracy

We discuss first the numerical accuracy of our calculation, and second the crucial approximations in our Hamiltonian and their effect on the reliability of the model.

Our calculation uses finite slabs of varying thicknesses [11 for the Cr (100) surface, 9 for the Cr monolayer on Fe (100), 7 for all (110) systems] to represent the metals and their surfaces. Comparison with calculations performed for the next thinner slab, e.g., nine layers for Cr (100), shows only a slight difference (less than 0.01 electron) in the surface spin polarization, thus suggesting adequate convergence with respect to slab thickness. It is important to note, however, that the central layer of the Cr slabs does not exhibit bulk spin polarization. We have found, by fixing the Cr polarization at the middle to extreme values (zero and the bulk moment 0.67), that this discrepancy does not influence the surface. Nonetheless, it is clear that some of our interior layers are altered by effects arising from two surfaces instead of just one.

Convergence with respect to wave-vector sampling is provided by 15 points evenly distributed throughout the irreducible (100)-surface Brillouin zone and 25 points evenly distributed throughout the irreducible (110) Brillouin zone. Evidence for the adequacy of this sampling was presented previously.[26]

We recapitulate now the crucial approximations in our Hamiltonian, and consider their effects. The use of a tight-binding scheme at surfaces produces several difficulties because it is unable to represent fully the nonspherical spilling of the electronic charge density into the vacuum. The resultant error in the charge transfer is handled in our scheme by the approximation (3), in which the self-consistent change in the potential is approximated by an on-site term, determined by imposing a zero-charge-transfer condition on the *sp*- and *d*-projected subbands separately at each site. Comparison with fully self-consistent calculations[22–24] suggests that this is an excellent approximation. Still the uncertainty of up to 0.1 electrons in the local *d* occupancy corresponds to a possible error of up to one tenth of a Bohr magneton, which may be measurable for Cr systems. However, there is no evidence that any available method is accurate to better than $0.1\mu_B$ for inhomogeneous systems. Approximation (3) also neglects the crystal-field splitting of the on-site potential.

Our tight-binding representation of charge densities also produces inaccuracies in the prediction of some Cr surface features in the spectra. Results of a detailed comparison with a chromium (100) photoemission experiment[27] suggest that we accurately predict the existence or absence of surface features and qualitatively predict the dispersion and intensities of those surface features. Errors in binding-energy prediction, however, may be as large as 0.05 Ry.

Even within the bulk the use of a tight-binding Hamiltonian should be analyzed with care. This method provides a good treatment of the *d* band, but the handling of the *sp* band is less accurate. Since *sp-d* hybridization plays an important role here, the tight-binding approximation introduces some risk of reduced quantitative accuracy.

Our Hartree-Fock treatment necessarily exaggerates the exchange splitting, which is reduced by correlation effects. Our restriction that the elemental Fe and Cr have the correct magnetic moment reduces the possible effects of this error. Nonetheless, it is possible that the exaggerated splitting may produce undesired consequences such as a slight distortion of the calculated density of states (DOS), which might make comparison with photoemission data more difficult.

Finally, it is important to note that, if many-body effects are important, the one-electron DOS which we calculate may not be the same as the excitation spectrum measured by photoemission. In particular, bulk Cr exhibits a slightly compressed (approximately 20%) photoionization spectrum[6] compared to the calculated DOS.

Ultimately we must base our assessment of overall accuracy upon comparison with reported results of fully self-consistent calculations for simple systems, and with experiment. Such comparisons are few, but they suggest that our methods reliably predict[26,28,29] the quantitative magnetization of heterogeneous systems. Other important conclusions that we draw either involve comparisons of different systems, in which case our errors should approximately cancel, or involve comparison with photoemission spectra, where our errors can be easily estimated.

III. RESULTS

In this section we discuss the results of our calculations and compare them with experiments and with other relevant calculations. In Secs. III A and III B we discuss the Cr (100) and the Cr (110) surfaces, respectively. The Cr monolayer on Fe, which is a model for the stainless-steel surface, is discussed in Sec. III C.

A. Chromium (100) surface

Our calculation gives a surface spin polarization of 3.00 electrons. This enhancement relative to the bulk, a factor of 5.1 from the SDW maximum, is much larger than that[26,29] found in Fe and Ni. The magnitude of the enhancement can be attributed to the large number of unpolarized *d* holes present in the bulk. Consequently, the decreased bandwidth found at the Cr surface, which leads to a stronger effective magnetic interaction, can greatly increase the surface spin polarization. Elements like Fe or Ni, with fewer available unpolarized holes, experience smaller changes in the same local environment.

The narrowing of the Cr DOS at the (100) surface is shown in Fig. 1. It is clear that most *d* holes occur in the minority subband. This subband is essentially concentrated in a single-peak structure entirely above the Fermi level. The surface DOS can be compared with the bulk DOS shown in Fig. 2. Here the *d* holes are almost evenly distributed between the two subbands. Furthermore, it is clear that both subbands have sizable strength on either side of the Fermi energy, which falls in a valley of the bcc DOS.

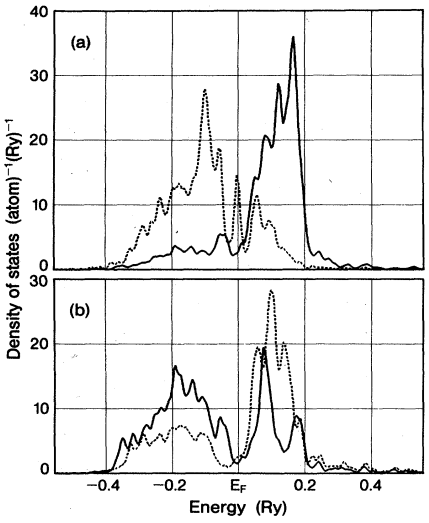

FIG. 1. The d orbital component of the projected density of states. (a) The chromium (100) surface layer. (b) The chromium (100) second layer. Solid lines are states with the spin orientation of the surface minority states; dashed lines correspond to the majority states.

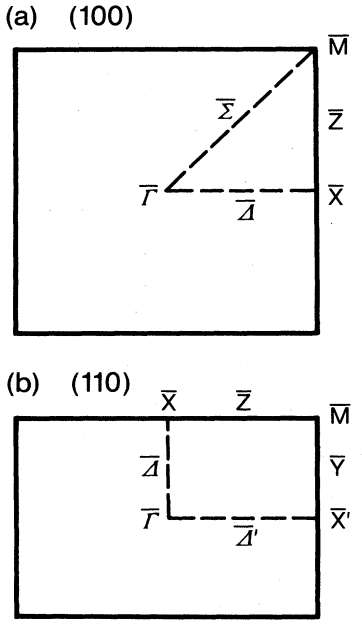

FIG. 3. Surface Brillouin zones.

Figure 1(b) shows the DOS projected at the layer immediately below the surface. The width of each subband is approximately equal to the bulk value, which is consistent with the presence of all nearest, and most second-nearest neighbors. The spin polarization is opposite to that of the surface layer, which is consistent with the AF of chromium. However, it is clear that there is a substantial difference between the minority and the majority DOS, suggesting that the spin polarization is not bulklike.

The spin polarization of the second layer is -1.56, substantially different from the bulk. The spin polarizations of the third through sixth layers are 1.00, -0.93, 0.86, and -0.85, respectively. A similar penetration of the enhanced surface magnetization was found in the Fe (100) surface,[26] although there the effect is much smaller. This penetration appears to be a direct consequence of the easy availability of unpolarized d holes in bulk Cr. Each atom feels the larger exchange splitting of its neighbor towards the surface and responds by increasing its own; this is, in the case of Cr, an energetically very inexpensive process.

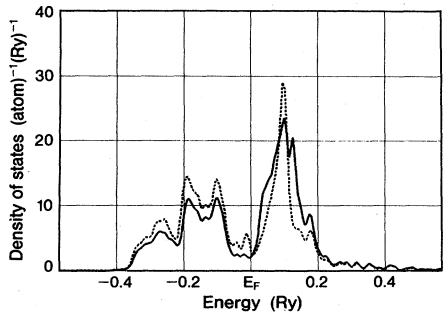

FIG. 2. The d orbital component of the bulk chromium density of states projected on one atom. Solid and dashed lines differentiate the two spin directions.

The (100)-surface Brillouin zone is shown in Fig. 3(a). Several points have high symmetry. In particular $\bar{\Gamma}$ and $\bar{M}$ have symmetry C_{4v} (see Table I), whereas $\bar{X}$ has symmetry C_{2v} (see Table II). All symmetry lines have the symmetry of a single reflection plane. At all points of high symmetry it is possible to have symmetry gaps, i.e., areas of the energy spectrum where no states of a given symmetry occur. In these symmetry gaps surface states of that symmetry may exist: they are states entirely located in the surface layers which make no connection with the bulk continuum. These surface states exist despite the absence of a true gap in the total density of states.

Figure 4 exhibits all states which are 60% localized within the two outermost layers on each side of our 11-layer slab. Normally states are localized mostly on the surface layer, but in this system the second layer is also unique: It is the layer with the highest polarization for spin direction opposite to that of the surface. It can therefore have its own localized states. The minority state of symmetry $\bar{\Gamma}_5$ is one example of such a state.

Table III lists those states at the symmetry points $\bar{\Gamma}$, $\bar{X}$, and $\bar{M}$ that are true surface states. The other states at these symmetry points are resonances, i.e., continuum

TABLE I. Character table for the point group C_{4v}.

Representation	E	C_2	$2C_4$	$2\sigma_v$	$2\sigma_d$
1	1	1	1	1	1
2	1	1	1	-1	-1
3	1	1	-1	1	-1
4	1	1	-1	-1	1
5	2	-2	0	0	0

TABLE II. Character table for the point group C_{2v}. Operation σ_v' is the reflection through the line perpendicular to $\mathbf{k}_{\bar{X}}$ in the (100) surface, and perpendicular to $\mathbf{k}_{\bar{X}'}$ in the (110) surface.

Representation	E	C_2	σ_v	σ_v'
1	1	1	1	1
2	1	1	−1	−1
3	1	−1	1	−1
4	1	−1	−1	1

states with a large amplitude at the surface.

One feature that may disturb the reader is that not all our surface states come in an exact twofold degeneracy arising from the two surfaces of the slab (the peaks at $\bar{\Gamma}$ above the Fermi energy are a clear example). The splitting is a consequence of the finiteness of the slab: The surface states of one surface are able to interact with their counterparts at the other surface.

The extensive agreement between our calculated surface electronic structure and the photoemission data of Klebanoff *et al.*[7] has been documented elsewhere.[27] Essentially it is found that the theoretical surface states of symmetry $\bar{\Gamma}_5$ correspond to the strong experimental surface feature of the same symmetry with a binding energy of 0.55 Ry. In particular, there is agreement with respect to intensities and dispersions along $\bar{\Delta}$. The theoretical surface state of symmetry $\bar{\Gamma}_1$, just above the Fermi level, probably corresponds to the experimentally observed feature at the Fermi level; the theoretical dispersion towards the Fermi level accounts for the observed intensity at nonzero surface **k** vector. The final two theoretical features at binding energies of 0.210 and 0.249 Ry are obscured from the experimental spectrum by the presence of a very strong bulk transition occurring near the same energy.

TABLE III. Surface states at special points of the (100)-surface Brillouin zone.

Label	Energy (Ry)
$\bar{\Gamma}(1\uparrow)$	+0.050
$\bar{\Gamma}(5\downarrow)$	−0.088
$\bar{\Gamma}(5\uparrow)$	−0.095
$\bar{\Gamma}(1\downarrow)$	−0.210
$\bar{M}(2\downarrow)$	+0.064
$\bar{M}(3\uparrow)$	+0.021
$\bar{M}(1\uparrow)$	−0.002
$\bar{M}(4\downarrow)$	−0.074
$\bar{M}(4\uparrow)$	−0.201
$\bar{M}(5\downarrow)$	−0.235
$\bar{M}(5\uparrow)$	−0.237

B. Chromium (110) surface

Our calculation gives a two-atom unit surface cell with AF ordering as the ground-state configuration. This configuration is in agreement with the simple saw cut of the bulk along the (110) plane. We were unable to find a ferromagnetic locally stable minimum in the ground-state energy. The surface spin polarization in the AF configuration is 2.31 electrons. This value is smaller than that for the (100) surface as one would expect, since the (110)-surface atom has six nearest neighbors, as opposed to four in the (100) surface. A larger bandwidth, suggested by the nearest-neighbor argument, is shown in Fig. 5(a).

Figure 5(b) shows the DOS projected on one of the second-layer atoms, a nearest neighbor to the atom in Fig. 5(a). As befits its nearest-neighbor status in an AF structure, the spin polarization is opposite to that of the surface atom. The spin polarization of 1.00 electrons is considerably smaller than that of a second-layer (100) atom, 1.56. It is a consequence not only of the smaller (110)-

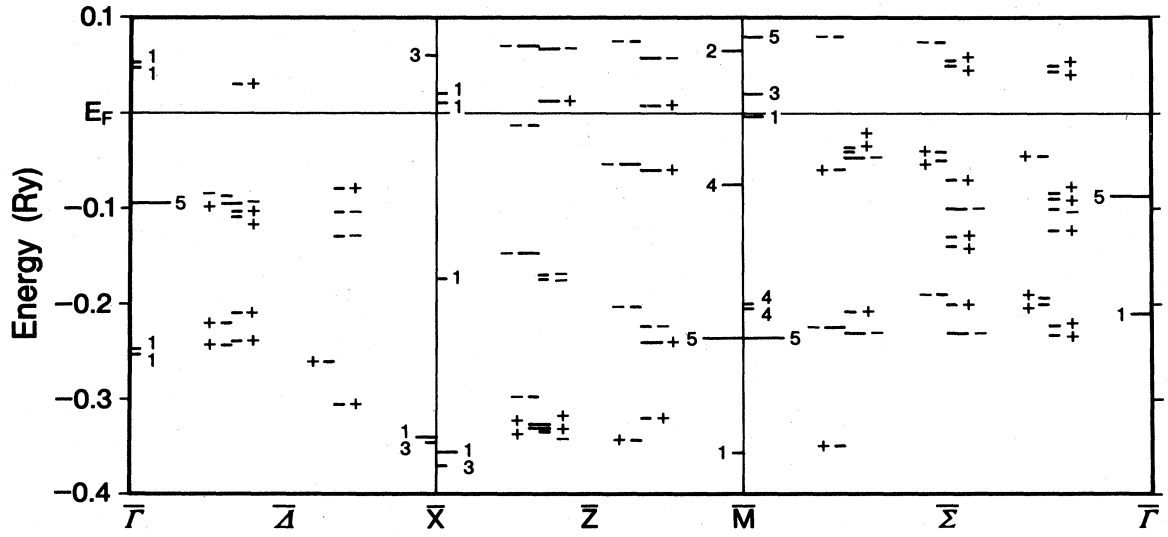

FIG. 4. Surface states and resonances at the Cr (100) surface. States shown to the right of a particular **k** vector are states with the spin orientation of the surface atom majority states; those shown to the left correspond to the minority states. The presence of two or four degenerate states is shown by the increased length of the marker.

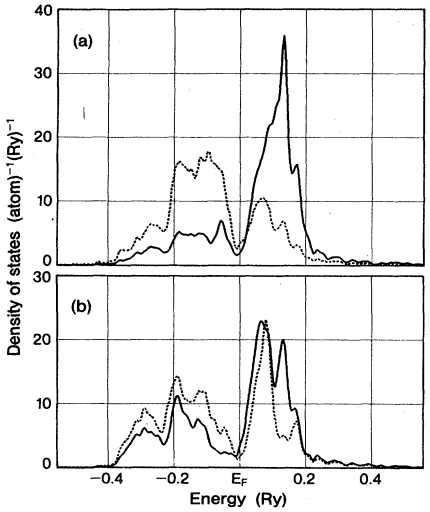

FIG. 5. The *d* orbital component of the density of states projected on one atom. (a) The chromium (110) surface layer. (b) The chromium (110) second layer. Solid and dashed lines differentiate the two spin directions.

surface perturbation, but also of the larger interlayer distance in the (110) direction. In particular, (100) layers are separated by $0.5a$ (where a is the lattice constant), whereas (110) layers are separated by $0.707a$, with a consequent smaller coupling between layers.

The (110)-surface Brillouin zone is shown in Fig. 3(b). The special points $\bar{\Gamma}$, $\bar{X}$, $\bar{M}$, and $\bar{X}$ all have symmetry C_{2v} (see Table II). The symmetry lines contain only a single mirror plane. Figure 6 indicates all states that are over 50% localized within the outermost layer. Note that the up- and down-spin eigenvalues are identical because of the complete AF of bulk and surface. However, the up- and down-spin features show different symmetries at some wave vectors. It is a consequence of the availability of two separate and distinct origins for the point-group operations.

There also exists experimental disagreement on photoemission spectra taken at the (110) $\bar{\Gamma}$ point. The data of Johansson *et al.*[14] show no surface features; those of Wincott *et al.*[15] show a state of presumed symmetry $\bar{\Sigma}_3$ which was measured from $\bar{\Gamma}$ to $\bar{X}$. The binding energy of this state, 0.011 to 0.022 Ry, is smaller than the one we find, but the dispersion is similar. In particular, we find the lowest binding energy, 0.053 Ry, to occur at approximately three quarters of the distance from $\bar{\Gamma}$ to $\bar{X}$, and for a local maximum to occur at the middle point. We find this state to be a resonance, not a surface state, because the $\bar{\Sigma}_3$ gap does not extend below the Fermi energy. Wincott *et al.*[15] find an AF periodicity equal to ours. We believe that their inability to find our surface feature of symmetry 1 is caused by the use of *s*-polarized light. (Symmetry 2 features at $\bar{\Gamma}$ are undetectable in photoemission.) In their paper, however, they do not state the precise polarization of their beam.

C. Chromium monolayer on iron

We have calculated the spin polarization of a Cr monolayer atop the Fe (100) surface to be 3.63 electrons, with a ferromagnetic arrangement pointing oppositely to the underlying Fe substrate. This value is the largest spin polarization we have ever calculated, or found in the literature, for a transition-metal system. It is interesting that it occurs for a system as important as the preoxidized stainless-steel surface. We were unable to obtain a local stable minimum for a Cr ferromagnetic layer, ferromagnetically ordered with respect to the iron.

Insight into this result may be gained by comparing it with the dilute *Fe*Cr alloy. Neutron scattering[30] results show that the isolated Cr atoms point oppositely to the

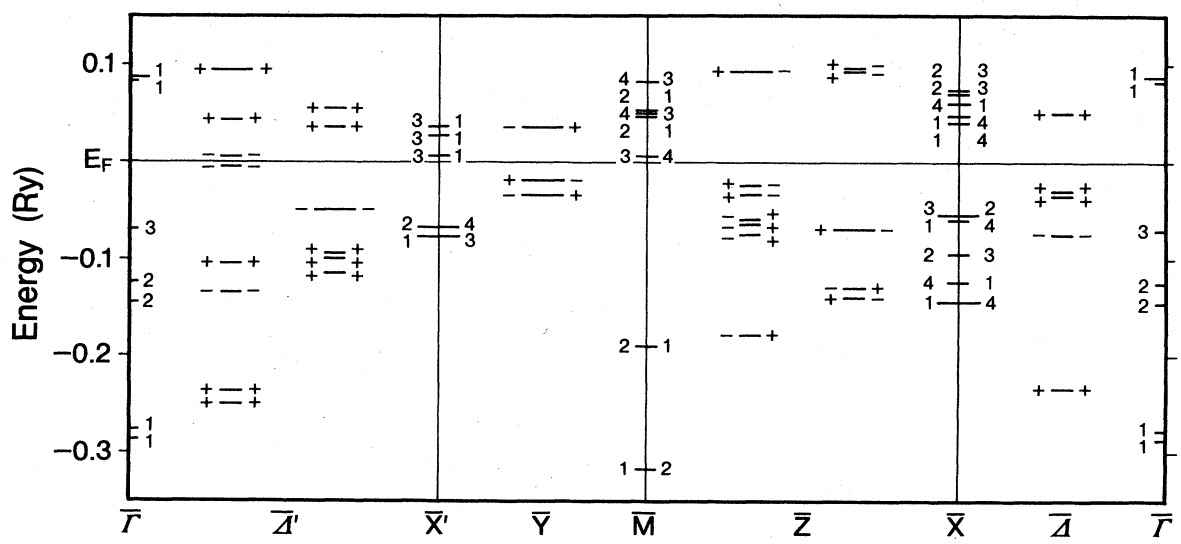

FIG. 6. Surface states and resonances at the Cr (110) surface. States shown to the immediate right of a particular **k** vector are states with one spin orientation; those to the left have the opposite spin. The presence of two degenerate states is shown by an increased length of the marker.

surrounding Fe bulk and have a spin polarization of 1.2 electrons, twice the maximum bulk value of the SDW. This latter result presumably stems from the stronger electron-electron interaction in Fe, and a consequent stronger exchange splitting which helps Cr increase its own splitting and magnetization. This is the same argument explored in great detail for the Fe-Co alloy[26], where Co has the stronger electron-electron interaction. The combined effect of diminished number of neighbors and stronger Fe exchange results in the calculated large Cr moment. We may understand the AF coupling by noting that Mn is the element intermediate between Fe and Cr, which suggests that the Fe-Cr interaction may be similar to the Mn-Mn interaction. Manganese exhibits localized moments but no ferromagnetism, implying that Fe and Cr would not couple ferromagnetically either. Figure 7 shows the DOS projected on the Cr monolayer and on the underlying Fe layer. The most obvious feature is the enormous minority DOS at the Cr monolayer (peak value of approximately 60/atom-Ry). It is a consequence not only of the surface band narrowing, but also of the absence of Fe majority holes to which the Cr minority holes (same spin) may be coupled. These two facts leave a subband with essentially no effective nearest neighbors, and therefore very narrow. The underlying Fe atoms are slightly affected by the Cr layer, and lower their spin polarization to 1.95 electrons.

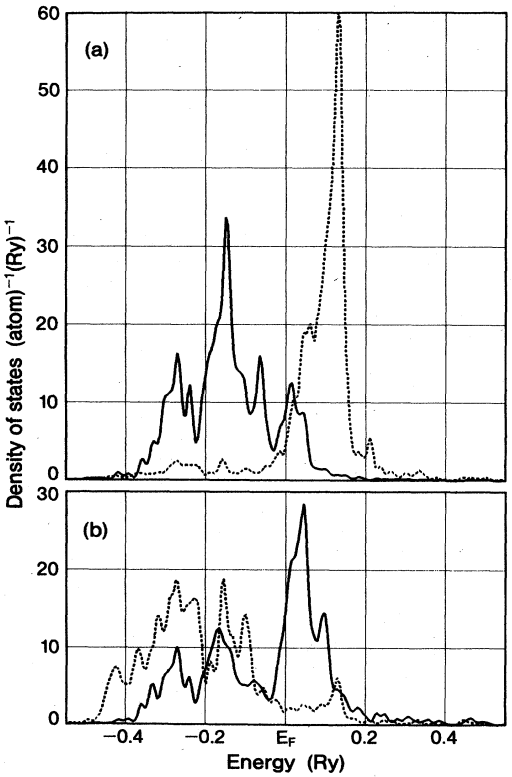

FIG. 7. The *d* orbital component of the projected density of states. (a) The chromium (100) monolayer. (b) The iron (100) interface layer. Solid lines are states with the spin orientation of the minority bulk iron states; dashed lines correspond to the majority states.

Consideration of a Cr monolayer atop the Fe (110) surface suggests several alternative configurations. One might expect the monolayer to be AF because of the AF interaction of each Cr atom with its four Cr neighbors. This arrangement forces half the Cr atoms to have a ferromagnetic interaction with the four underlying nearest Fe atoms. As already discussed, Fe has a very strong effect on the Cr spin polarization (it doubles the value of the Cr polarization in the dilute alloy). The Fe substrate therefore would favor a ferromagnetic Cr monolayer, with AF order with respect to the bulk. Clearly there are two competing effects, and the nature of the ground state can be determined only after a detailed calculation.

We find that the ground state consists of a ferromagnetic Cr monolayer with its spins oriented in the direction opposite to the Fe substrate, similar to the Cr-on-Fe (100) arrangement. The spin polarization of the Cr is 2.25 electrons, smaller than the pure Cr surface. There is, as in the (100) monolayer, a small decrease in the spin polarization of the underlying Fe layer to a value of 2.03 electrons. The projected DOS at the Cr layer and at the underlying Fe layer is shown in Fig. 8. Changes from the bulk DOS are not spectacular and mostly they reflect just the increased spin polarization.

We find that a structure consisting of an AF chromium layer is metastable: It produces a local minimum in the total energy curve, 0.05 Ry/surface atom above the ground state. The spin polarizations of the two different Cr atoms are 3.03 and -3.31 electrons, with the larger magnitude corresponding to the atom with AF arrangement to both its Cr and Fe nearest neighbors. It is clear that because of the different magnitudes of the spin polarizations the Cr monolayer is not truly AF, but rather ferrimagnetic. One finds in the projected DOS (Fig. 9) a narrow and tall minority-hole peak on the second atom for much the same reasons as those given for the (100) monolayer results.

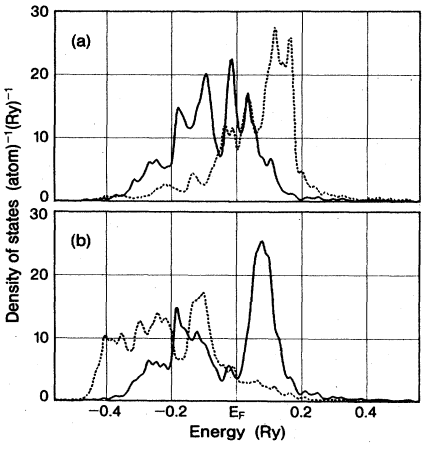

FIG. 8. The *d* orbital component of the projected density of states. (a) Ground state, the Cr (110) monolayer. (b) Ground state, the Fe (110) interface layer. Solid lines are states with the spin orientation of the minority bulk iron states; dashed lines correspond to the majority states.

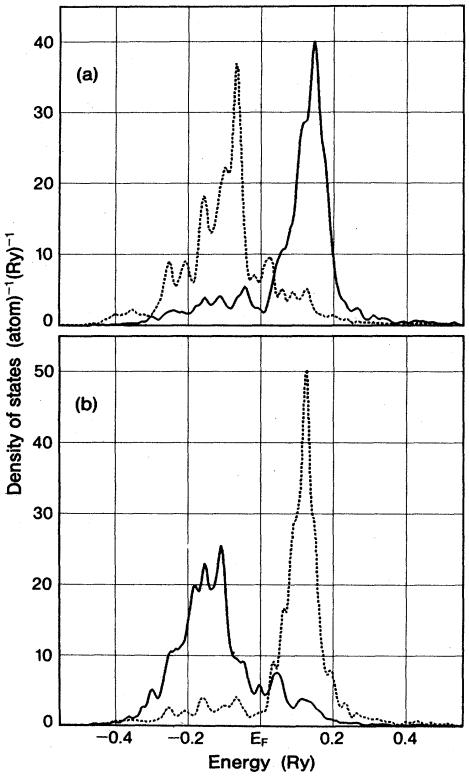

FIG. 9. The *d* orbital component of the projected density of states for the antiferromagnetic chromium monolayer on iron (110). (a) Chromium atom with the iron spin orientation. (b) Chromium atom with spin pointing oppositely to the iron spin direction. Solid lines are states with the spin orientation of the minority bulk iron states; dashed lines correspond to the majority states.

IV. CONCLUSION

The (100) surface of Cr is found to be ferromagnetic with a spin polarization of 3.00 electrons, whereas the (110) surface is found to be AF. Both magnetic configurations are in agreement with experiment and constitute the configuration of the (100) and (110) planes in the commensurable AF bulk structure. At both surfaces there is considerable penetration of the greatly enhanced surface magnetization into the bulk. Both the large surface spin polarization and the penetration may be understood as consequences of the large number of *d* holes available for spin polarization. A very strong surface state of symmetry $\bar{\Gamma}_5$ is found at the center of the (100)-surface Brillouin zone. This is in agreement with a recent photoemission experiment in Cr.

Chromium monolayers on Fe are found to be ferromagnetic, with the Cr spins aligned in the opposite direction to the Fe spins. At the (110) surface this arrangement forces Cr nearest neighbors to have the same spin direction, a result which indicates the strength of the Fe-Cr interaction. The (100) Cr monolayer possesses the largest spin polarization for a transition-metal system known to the authors. This polarization, 3.63 electrons, is caused by the combination of (100)-surface-band narrowing and the strong antiferromagnetic Fe-Cr interaction.

Many predictions made here regarding magnetic configurations could be easily tested by photoemission experiments. In particular x-ray spin-polarized photoemission could easily check the antiparallel arrangement of the Cr and Fe spins, since the Cr core levels should order their excitation energies oppositely to those of Fe. Enhanced magnetization of the Cr surfaces could be deduced from the increased differences between the up- and the down-spin excitation energies relative to those in the bulk. We hope that our results will stimulate additional experimental work aimed at determining the behavior of these extremely magnetic systems.

ACKNOWLEDGMENTS

We would like to thank L. E. Klebanoff and J. W. Morris for providing us with unpublished information and for enlightening discussions at various stages of this work. One of us (R.H.V.) would like to acknowledge support by AT&T Bell Laboratories, under whose sponsorship this research was done. This work was supported by the Director, Office of Energy Research, Materials Science Division of the U. S. Department of Energy, under Contract No. DE-AC03-76SF00098.

[1]C. Kittel, *Introduction to Solid State Physics,* 5th edition (Wiley, New York, 1976), p. 465.
[2]S. A. Werner, A. Arrott, and H. Kendrick, Phys. Rev. **155**, 528 (1967).
[3]G. Shirane and W. J. Takei, J. Phys. Soc. Jpn. **17**, Suppl. (BIII), 35 (1962).
[4]W. C. Koehler, R. M. Moon, A. L. Trego, and A. R. Mackintosh, Phys. Rev. **151**, 405 (1966).
[5]C. Rau and S. Eichner, Phys. Rev. Lett. **47**, 939 (1981).
[6]G. Gewinner, J. C. Peruchetti, A. Jaéglé, and R. Pinchaux, Phys. Rev. B **27**, 3358 (1983).
[7]L. E. Klebanoff, S. W. Robey, G. Liu, and D. A. Shirley, Phys. Rev. B **30**, 1048 (1984).
[8]L. E. Klebanoff (private communication).
[9]G. Allan, Surf. Sci. **74**, 79 (1978).
[10]G. Allan, Phys. Rev. B **19**, 4774 (1979).
[11]D. R. Grempel, Phys. Rev. B **24**, 3928 (1981).
[12]P. J. Feibelman and D. R. Hamann, Phys. Rev. B **31**, 1154 (1985).
[13]M. B. Brodsky, P. Marikar, R. J. Friddle, L. Singer, and C. H. Sowers, Solid State Commun. **42**, 675 (1982).
[14]L. I. Johansson, L. G. Petersson, K. F. Berggren, and J. W. Allen, Phys. Rev. B **22**, 3294 (1980).
[15]P. L. Wincott, N. B. Brookes, D. S. Law, G. Thornton, and H. A. Padmore, Vacuum **33**, 815 (1983).
[16]G. Betz, G. K. Wehner, L. Toth, and A. Joshi, J. Appl. Phys. **45**, 5312 (1974).
[17]*CRC Handbook of Chemistry and Physics,* 53rd edition

(Chemical Rubber, Cleveland, 1972), p. F-188.
[18]J. C. Slater and G. F. Koster, Phys. Rev. **94**, 1498 (1954).
[19]V. L. Moruzzi, J. F. Janak, and A. R. Williams, *Calculated Electronic Properties of Metals* (Pergamon, New York, 1983).
[20]C. Herring, in *Exchange Interactions Among Itinerant Electrons,* Vol. IV of *Magnetism,* edited by G. T. Rado and H. Suhl (Academic, New York, 1966), and references therein.
[21]C. Herring, Ref. 20, p. 227.
[22]H. Krakauer, A. J. Freeman, and E. Wimmer, Phys. Rev. B **28**, 610 (1983).
[23]S. Onishi, A. J. Freeman, and M. Weinert, Phys. Rev. B **28**, 6741 (1983).
[24]J. Noffke and L. Fritsche, J. Phys. C **14**, 89 (1981).
[25]E. Merzbacher, *Quantum Mechanics,* 2nd edition (Wiley, New York, 1970), p. 538.
[26]R. H. Victora, L. M. Falicov, and S. Ishida, Phys. Rev. B **30**, 3896 (1984).
[27]L. E. Klebanoff, R. H. Victora, L. M. Falicov, and D. A. Shirley, Phys. Rev. B (to be published).
[28]R. H. Victora and L. M. Falicov, Phys. Rev. B **30**, 259 (1984).
[29]J. Tersoff and L. M. Falicov, Phys. Rev. B **26**, 6186 (1982).
[30]A. T. Alfred, B. D. Rainford, J. S. Kouvel, and T. J. Hicks, Phys. Rev. B **14**, 228 (1976).